J Solid State Electrochem (2007) 11:150–154
DOI 10.1007/s10008-006-0214-z

ORIGINAL PAPER

A new SERS-active sandwich structure

Yongan Yang · Alexander M. Bittner · Klaus Kern

Received: 24 November 2005 / Revised: 31 January 2006 / Accepted: 23 February 2006 / Published online: 25 October 2006
© Springer-Verlag 2006

Abstract We report surface-enhanced Raman scattering (SERS) from a "sandwich" structure of two silver layers, in which a thin film of activated carbon is embedded. The first silver layer is prepared by electroless deposition on a non-conductive substrate, while the second one is electrodeposited on the adsorbed carbon powder. This "sandwich" does not only yield stable SERS signals from the carbon but also a strong additional enhancement (compared to SERS from simple carbon/silver or silver/carbon structures), stemming from a coupling of the two silver layers. The "sandwich" structure should be widely applicable since its preparation is very simple.

Keywords Surface-enhanced Raman scattering (SERS) · Porous carbon electrodes · Activated carbon · Electrochemical double-layer capacitors

Introduction

Surface-enhanced Raman scattering (SERS) is a method for obtaining Raman spectra—and in this way, for example, molecular vibrations—from a very small amount of scatterers that are adsorbed on a specially designed surface [1–3]. The drastic enhancement—Raman signals of an adsorbate can increase by several orders of magnitude on certain substrates—makes SERS a powerful tool to analyze a range of diverse specimens, e.g., materials [4], biomolecules [5], environmentally important molecules [6], and catalysts [7]. In 1997, Nie and Emory [8, 9] and Kneipp et al. [10] demonstrated the detection of single molecules. SERS is believed to result from two contributions, originally proposed two decades ago [11, 12]: the electromagnetic field mechanism (based on surface plasma resonance) and the chemical bonding mechanism, but the detailed mechanism is still under debate [13, 14].

Various methods have been developed to produce SERS-active substrates: electrochemical roughening of electrodes [15], electrodeposition [16], fabrication of colloidal particles [17], vacuum deposition [18], pyrolysis of organometallic salts [19], and chemical reduction [20–23]. While SERS originates usually from the adsorbate/substrate interface, it is also possible to prepare a SERS-active metal layer on molecules adsorbed on a non-active substrate, although a relatively low enhancement is observed [24, 25]. Only recently, several groups developed "sandwich" structures consisting of either two colloidal particle layers or one thin film and one colloid layer, with the adsorbate being embedded between the layers [26–28]. A sandwich configuration should help to obtain even higher enhancement, as the adsorbate is surrounded by metallic structures in multiple directions. When cytochrome is embedded in a silver colloid sandwich, SERS is four times stronger than a single-substrate structure [26]. Benzoic acid in multilayered silver films shows extra enhancement, too [29], and even a three-layer film technique (gold and silver) was developed [30].

Paper presented at the "Jahrestagung der Fachgruppe Angewandte Electrochemie der Gesellschaft Deutscher Chemiker, Düsseldorf, 11.–14.06.2005."

Y. Yang (✉) · A. M. Bittner (✉) · K. Kern
Max-Planck-Institute for Solid State Research,
Heisenbergstr. 1,
70569 Stuttgart, Germany
e-mail: yonganyang@chem.ufl.edu
e-mail: a.bittner@fkf.mpg.de

Present address:
Y. Yang
Department of Chemistry, University of Florida,
Gainesville, FL, USA

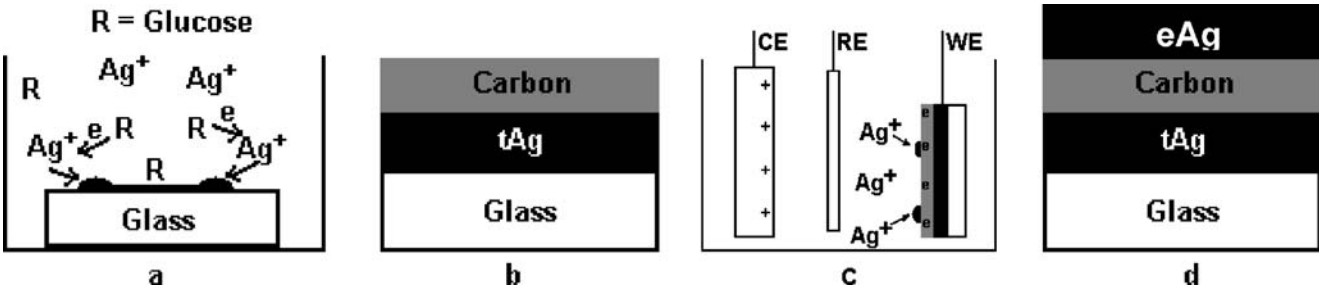

Fig. 1 Simple procedure for a SERS-active "sandwich" structure. **a** tAg/glass, electroless deposition of silver (Tollens reaction) on glass or other substrates; **b** C/tAg/glass, adsorption of Raman scatterer (carbon powder); **c** eAg/C/tAg/glass, electrodeposition of silver under potentiostatic control with tAg as working electrode; **d** eAg/C/tAg/glass, final structure

In this paper, we report a sandwich structure of two silver layers, embedding activated carbon (see Fig. 1), which exhibits stable and strong SERS. SERS of various carbon allotropes is well documented [31–35]; carbon is also an excellent source for stable unenhanced Raman bands, and carbon powder (activated carbon) can easily adsorb on glass and metals; hence, we employed it as reference substance. The highly activated porous carbon that we used as Raman scatterer has a large range of applications, amongst them is its use as electrode material in electrochemical double-layer capacitors. During the activation process, some oxygen-based surface functional groups inside the carbon grains are produced. In addition, a very large fraction of the carbon atoms are present as surface atoms in pores. These atoms are accessible for gases, liquids, and not-too-large ions, resulting in an extremely high capacitance of the electrodes. Despite the complex structure of porous carbon, its Raman spectrum is simple, and the interpretation is straightforward. While Raman spectra are well known from all types of carbon materials, SERS is best known from carbon nanotubes since they show an inherent enhancement [31–35], which had to be avoided in our study.

The underlying silver layer, "tAg", was produced by the Tollens reaction (electroless deposition) [20], and the silver layer atop the carbon, "eAg", was electrochemically deposited from aqueous Ag^+ on the carbon-coated silver substrate (Fig. 1). The sandwich structure shows a much higher SERS intensity than the individual Tollens silver layer. We thus demonstrate cooperative coupling between two SERS-active silver layers.

Experimental

The Tollens reaction [reduction of aqueous $Ag(NH_3)_2^+$ by glucose] that we employed to produce the 2-μm-thick "tAg" layer was adapted from [20]. Ten drops of 5% NaOH (p.A., Merck) solution were added to 10 ml of ice-cooled 2–3% $AgNO_3$ (p.A., Merck) solution. Subsequently, concentrated ammonia solution (30%, Selectipur, Merck) was added dropwise until the brown precipitate produced in the first step disappeared. The glass substrates, cleaned by concentrated HNO_3, were then immersed. Three milliliters of 10% glucose solution (Caelo) were added, and the mixture was warmed to 25 °C. It was then heated to 50 °C for 10 min, and ultrasonicated for 1 min. The thus produced tAg/glass samples were rinsed with copious amounts of pure water.

The activated carbon powder (see Fig. 2a; type "PKC"; specific area, 1,150 cm^2/g; CarboTech) was mechanically pressed onto the glass or silver surfaces as a 50- to 500-nm-thin film. The electrodeposition setup for producing the eAg layer employed platinum counter and reference electrodes. The electrolyte solution was 10 mM $AgNO_3$+100 mM Na_2SO_4 (p.A., Merck), adjusted to pH=8–9 by $NH_3{\cdot}H_2O$. The electrodeposition of silver was performed with an Autolab potentiostat by recording two cycles of a voltammogram between 0 and −500 mV at a scan rate of 20 mV/s (the potentials refer to a Pt wire, which—due to spontaneous deposition of Ag—quickly attains the Ag/Ag^+ equilibrium of 680 mV_{SHE}). Note that the eAg layer is not a continuous film but consists of discrete grains. Given a coverage of about 80%, the average thickness of the layer is estimated to 2 nm based on evaluating the cyclic voltammogram (see Fig. 2b), the electroplating area, and the Ag atomic data. Raman experiments were performed with a Jobin Yvon Labram spectrometer under normal incidence (1 mW, 632.8 nm), and the scattered light was collected with a ×50 objective. The spectra were acquired with various exposure times from 1 to 100 s but are here presented normalized to 1 s for better comparison. Atomic force microscopy (AFM) images were recorded with a Nanoscope IIIA (Digital Instruments) operated in tapping mode (280 to 300 kHz) with silicon tips. Roughness values were obtained by conventional averaging as root of mean squares (rms).

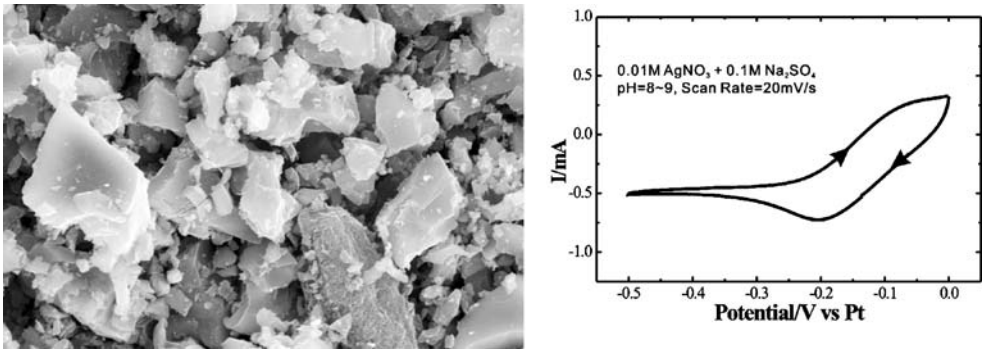

Fig. 2 **a** Scanning electron micrograph of the employed activated carbon; image size, 56 μm×37 μm. **b** Cyclic voltammogram for the electrodeposition of silver (eAg layer) on a C/tAg substrate

Results and discussions

Figure 3a shows Raman spectra of activated carbon for three different layered structures (C/tAg/glass, C/eAg/tAg/glass, and eAg/C/tAg/glass), together with a spectrum of an activated carbon layer on glass (C/glass) for comparison. C/eAg/tAg/glass can be produced by exchanging the last two steps in forming eAg/C/tAg/glass. Clearly, all three structures show a remarkable signal enhancement compared to the C/glass structure that is taken as reference (no enhancement). Note that all the spectra were, for the sake of comparability and good signal/noise ratio, acquired with the same parameters (e.g., laser power, filter aperture, objective, etc.), except for the accumulation time. The thickness of the carbon layers was in the range of 50 to 500 nm. The observed Raman peak at 1,596 cm^{-1} is assigned to the so-called G-band, originating from the E_{2g} stretching mode in the graphene basal plane [36], and the peak at 1,326 cm^{-1} is attributed to the D-band, arising from disorder-induced k-nonconserving scattering, resonant at intermediate states [37]. Even with the help of the sandwich structure, it seems still impossible to identify further bands, e.g., those from the very small number of functional groups. The intensity of the C/glass spectrum is weak, and the fluorescent background from the glass substrate distorts the profile. When the glass was first coated by electroless silver, tAg, the corresponding Raman signal of the carbon increased 33-fold (this enhancement factor is the ratio between the integrated peak intensity of the D-band to that of the D-band in C/glass). In comparison with the ordinary enhancement factor for organic molecules (10^4 to 10^6), 33 appears very small. However, only a tiny amount of the carbon adsorbed on the silver particles can be accessed by the enhanced electric field around a silver cluster (which extends some tens of nm); hence, the true enhancement factor must be higher than the nominal value of 33. The reason is that the activated carbon we employed has a rather broad size distribution. Particle sizes range from sub-micrometer to several nanometers (some big chunks measure 20 μm), with two main groups at <1 and 2–5 μm. In SEM images (Fig. 2a), particles overlap substantially, so the thickness is hard to measure; overall, the particles are more flake-like and less than 1 μm thick. All these properties are responsible for the small contact area between carbon and silver particles.

When another silver layer (eAg) was electrodeposited on the carbon, the enhancement factor amounted to 710 (for SERS of diamond on silver particles [24] and for amorphous carbon evaporated on silver particles [38], this value is ~100). Considering a possible loss of carbon, the actual enhancement might be even much higher. While the enhancement is far from optimal, the intriguing point is the large *additional* enhancement (20-fold) after completion of the sandwich structure (eAg/C/tAg/glass compared to C/tAg/glass). In order to confirm the sandwich effect, we also studied a reference structure, C/eAg/tAg/glass (the electrodeposition conditions of the eAg layer were the same as that of eAg in eAg/C/tAg). The measured enhancement was 238, much larger than that of C/tAg/glass but far below that of eAg/C/tAg/glass, as shown in Fig. 3b. Whether the

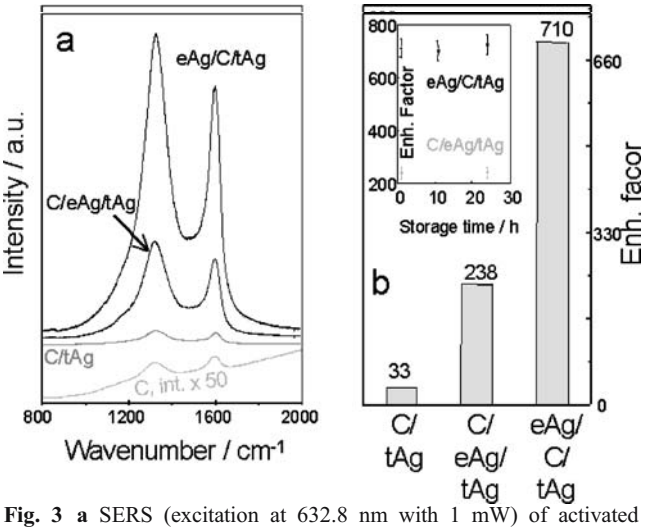

Fig. 3 **a** SERS (excitation at 632.8 nm with 1 mW) of activated carbon in various structures. The spectra are offset for clarity. Electroless silver (Tollens reaction) is denoted by *tAg* and electrodeposited silver by *eAg*. *eAg/C/tAg/glass* is the sandwich structure. **b** Relative enhancement, normalized to C/glass. *Inset*: stability of SERS from eAg/C/tAg/glass (*black*, sandwich structure) and from C/eAg/tAg/glass (*gray*). The integrated peak intensity refers to C/glass

tAg layer also plays a role here is not clear. If there is no contribution from the tAg layer, the pure contribution from the eAg layer is 238. If the tAg layer does contribute to some extent, the enhancement by the eAg layer will become *even less* than 238 (this seems not the case, considering that SERS arises from the resonance of *surface* plasmons and that the effective surface here is linked to the morphology of the eAg layer). In any case, the maximum enhancement by the eAg layer alone is merely 238.

Usually SERS-active layers atop a scatterer give lower enhancement than a scatterer adsorbed on a SERS-active substrate. Hence, the eAg layer-based enhancement for eAg/C/tAg should be less than 238, provided that these two layers contribute individually without coupling to each other. But in fact, we observed an enhancement of 710. This means that a simple additive effect of eAg and tAg can *not* explain the sandwich SERS, and a coupling effect is needed to account for the additional SERS effect. Besides that, our structures (and also C/tAg/glass) exhibit a very stable level of SERS without loss of enhancement for at least 2 days (see Fig. 3b inset). The 5 and 9% error bars clearly indicate the good reproducibility. Stability is one of the most important issues for SERS substrate performance (SERS from silver islands on glassy carbon can vanish within minutes [16]), and it is crucial for sandwich structures.

In contrast to our stable and relatively high enhancement, silver colloid-based sandwich structures of cytochrome have a relative enhancement (Ag/cytochrome/Ag vs cytochrome/Ag) of only 4 at 488 nm excitation [26]. If interpolated according to Fig. 12 in [26], the value is only ~0.2 at 633 nm (the wavelength we used); i.e., the respective sandwich structure shows no additional enhancement, but a reduction. A related system, silver particles/azobenzene/gold [27], shows a relative enhancement (maximum of 560) comparable to our results. Zheng et. al. [28] studied the system silver colloids/aminothiol/smooth silver without reporting an enhancement factor. In all three studies [26–28], either the sandwich structure has no big advantage, or the underlying substrate is SERS-inactive. Recently, more complex procedures have been developed: Li and Cullum [29] showed that multiple silver layers over nanostructured films can improve single layer performance, and Mulvaney et al. [30] introduced a three-layer system. We here present a simple and stable sandwich structure with a high *cooperative coupling effect*, for which two SERS-active silver layers were designed. The local arrangement of the metal particles, rather than their mere amount, is decisive [13, 14].

AFM can give some insight into the particle arrangement in our samples. Figure 4 shows the morphology of three SERS-active substrates, all acquired in tapping mode AFM. The tapping insures that all surface feature heights are properly scanned, while the width of small features (<50 nm) can appear enlarged (depending on the size of

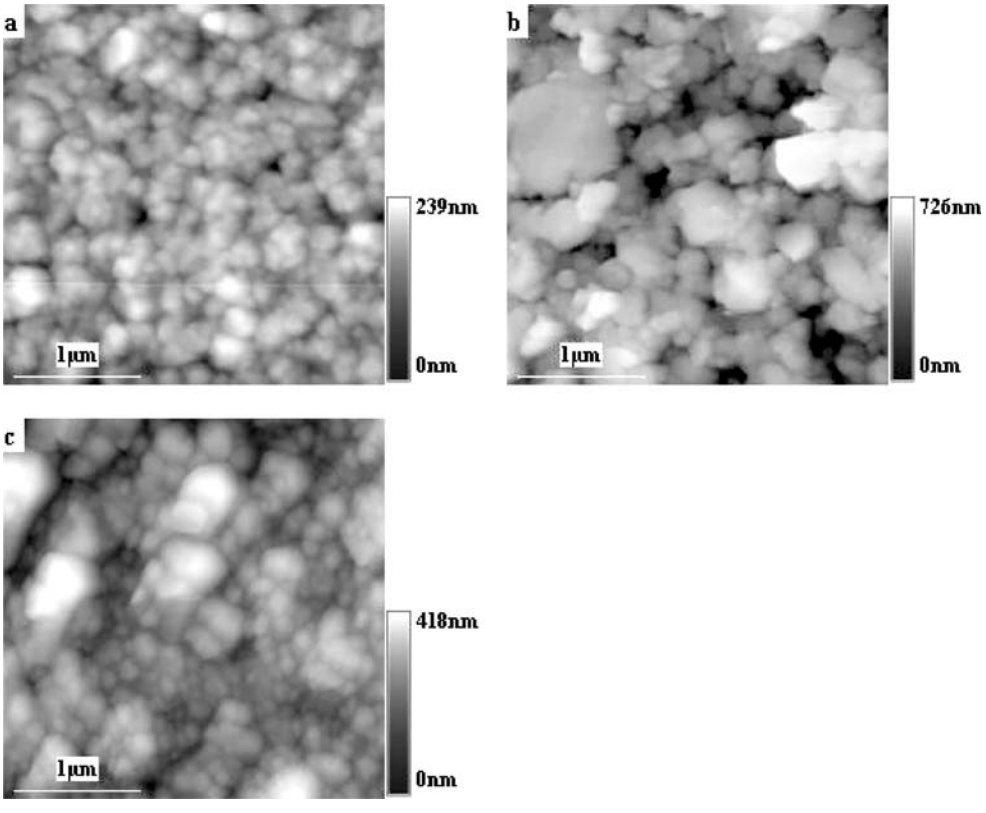

Fig. 4 The morphology of **a** tAg/glass, **b** eAg/tAg/glass, and **c** eAg/C/tAg/glass, recorded by tapping mode atomic AFM

the AFM tip). Note that it was impossible to measure the sizes of individual particles since the particles coalesced to a large extent, and their boundaries vanished or appeared blurred. The tAg surface (Fig. 4a) was quite uniform with an rms roughness value of 27±1 nm on 9 μm^2, and with particle sizes of ~100 nm. Conversely, shown in Fig. 4b, the surface of eAg/tAg/glass became rougher (rms=76± 4 nm on 9 μm^2) with an increase of the particle sizes originating from electrodeposition. The eAg/C/tAg/glass surface (Fig. 4c) yielded similar magnitudes of the particle sizes and of the rms roughness (65±5 nm on 9 μm^2). Simulations for single SERS-active substrates predict that the electric field enhancement is strongly roughness-dependent [39], which might suggest to interpret the enhancement difference between eAg and tAg layers. However, comparisons between eAg/tAg and eAg/C/tAg (both have similar roughnesses) clearly show that our sandwich structure, rather than the roughness, is the essential factor accounting for the large additional enhancement (cooperative coupling).

So far, we have not considered the possibility that silver particles not only cover the carbon grains from top and/or bottom but also *surround* them laterally. Our conclusion concerning the coupling effect would then remain valid since this morphology exists on each silver layer, and the essential difference between eAg/C/tAg and other systems is still the sandwich structure. Unfortunately, it is impossible to distinguish carbon particles from silver particles. It should be stressed that the sandwich structure here is much more complex than theoretical models. Although exhaustive mechanistic understanding of this extra-enhancement requires further experiments and a rather complex model, it is very likely due to electromagnetic fields between the nanoparticle layers, resulting from enhanced surface plasmon resonances [37].

Summary

We have shown that it is possible to observe strong SERS from porous activated carbon "sandwiched" between two silver layers. For this we prepared rough silver layers with two simple techniques: electroless deposition followed by electrodeposition. Embedding the sample between the electroless and electrodeposited silver layers ("sandwich structure", by adsorbing the sample before the electrodeposition) leads to a cooperative coupling effect, i.e., to a large additional enhancement over to the sum of two simple carbon/silver structures. The sandwich-based SERS is remarkably stable, and many molecular species should also qualify as scatterers. Especially because electroless silver does not require conductive surfaces, sandwich-based SERS could thus become a widely applied method.

Acknowledgments We thank Annette Fuchs for preparing the SEM micrograph and Manxi Zhu for helpful discussions.

References

1. Fleischmann M, Hendra PJ, McQiullan AM (1974) Chem Phys Lett 26:163
2. Mulvaney SP, Keating CD (2000) Anal Chem 72:145R
3. Campion A, Kambhampati P (1998) Chem Soc Rev 27:241
4. Duesberg GS, Blau WJ, Byrne HJ, Muster J, Burghard M, Roth S (1999) Chem Phys Lett 310:8
5. Keating CD, Kovaleski KK, Natan MJ (1998) J Phys Chem B 102:9404
6. Liang EJ, Yang Y, Kiefer W (1999) Spectrosc Lett 32:689
7. Petersen P, Krasser W (1996) Appl Surf Sci 103:91
8. Nie S, Emory SR (1997) Science 275:1102
9. Doering WE, Nie S (2002) J Phys Chem B 106:311
10. Kneipp K, Wang Y, Kneip H, Perelman LT, Itzkan I, Dasari RR, Feld M (1997) Phys Rev Lett 78:1667
11. Jeanmaire DL, Van Duyne RP (1977) J Electroanal Chem 84:1
12. Albrecht MG, Creighton GA (1977) J Am Chem Soc 99:5215
13. Michaels AM, Jiang J, Brus L (2000) J Phys Chem B 104: 11965
14. Jiang J, Bosnick K, Maillard M, Brus L (2003) J Phys Chem B 107:9964
15. Mrozek MF, Wasileski SA, Weaver MJ (2001) J Am Chem Soc 123:12817
16. Alsmeyer YW, McCreery RL (1991) Anal Chem 63:1289
17. Lee PC, Melsel D (1982) J Phys Chem 86:3391
18. Schlegel VL, Cotton TM (1991) Anal Chem 63:241
19. Lee SJ, Kim K (2003) Chem Commun 212
20. Ni F, Cotton TM (1986) Anal Chem 58:3159
21. Leopold N, Lendl B (2003) J Phys Chem B 107:5723
22. Saito Y, Wang JJ, Smith DA, Batchelder DN (2002) Langmuir 18:2959
23. Bittner A, Wanner M, Weil KG (1992) Ber Bunsenges Phys Chem 96:647
24. Roy D, Barber ZH, Clyne TW (2002) J Appl Phys 91:6085
25. Lopez-Rios T (1996) Diamond and Related Materials 5:608
26. Keating CD, Kovaleski KK, Natan MJ (1998) J Phys Chem B 102:9414
27. Yu H, Zhang J, Zhang H, Liu Z (1999) Langmuir 15:16
28. Zheng J, Zhou Y, Li X, Lu T, Gu R (2003) Langmuir 19:632
29. Li H, Cullum BM (2005) Appl Spectrosc 59:410
30. Mulvaney SP, He L, Natan MJ, Keating CD (2003) J Raman Spectrosc 34:163
31. Zoval JV, Biermacki PR, Penner RM (1996) Anal Chem 68: 1585
32. Siu GG, Liu Y, Xie S, Xu J, Li T, Xu L (1996) Thin Solid Films 274:147
33. Corio P, Brown SDM, Marucci A, Pimenta MA, Kneipp K, Dresselhaus G, Dresselhaus MS (2000) Phys Rev B 61:13202
34. Itoh T, Abe K, Mahamedi M, Nishizawa M, Uchida I (2001) J Solid State Electrochem 5:328
35. Mews A, Koberling F, Basché T, Philipp G, Duesberg GS, Roth S, Burghard M (2000) Adv Mater 12:1210
36. Pocsik I, Hundhausen M, Koos M, Ley L (1998) J Non-cryst Solids 1083:227–230
37. Matthews MJ, Pimenta MA, Dresselhaus G, Dresselhaus MS, Endo M (1999) Phys Rev B 59:6585
38. Ilie A, Durkan C, Milne WI, Welland ME (2002) Phys Rev B 66:045412
39. Garcia-Vidal FJ, Pendry JB (1996) Phys Rev Lett 77:1163